Available online at www.sciencedirect.com
SCIENCE DIRECT®
ELSEVIER
Applied Surface Science 208–209 (2003) 45–51
applied surface science
www.elsevier.com/locate/apsusc

Analysis of the plasma produced by pulsed reactive crossed-beam laser ablation of $La_{0.6}Ca_{0.4}CoO_3$

M.J. Montenegro[a], C. Clerc[b], T. Lippert[a,*], S. Müller[c], P.R. Willmott[a,b], A. Weidenkaff[d], A. Wokaun[a]

[a]*Paul Scherrer Institute, CH-5232 Villigen PSI, Switzerland*
[b]*Physical Chemistry Institute, University of Zürich, Winterthurerstr, 190 CH-8057 Zürich, Switzerland*
[c]*Euresearch, Effingerstr, 19 CH-3001 Bern, Switzerland*
[d]*University of Augsburg, Universitätstr, 1 D-86159 Augsburg, Germany*

Abstract

Pulsed laser deposition (PLD) in conjunction with a synchronized pulsed gas source provides an extra degree of freedom in processing the ablation plume. This technique is called pulsed reactive crossed-beam laser ablation (PRCLA). The ablation plasma of $La_{0.6}Ca_{0.4}CoO_3$ (LCCO) produced by KrF excimer laser (248 nm) irradiation is analyzed by spatially and temporal resolved optical emission spectroscopy in the range of 300–800 nm in vacuum, with oxygen background and with an additional N_2O as a gas pulse. The spectra reveal higher intensities for all the peaks when the gas pulse is applied. No new peaks assigned to the interaction with the gas pulse, i.e. oxygen, nitrogen or diatomic species are observed. The maximum intensities of the plasma with the gas pulse are observed later in time and further away from the target.

Keywords: Pulsed reactive crossed-beam laser ablation; Perovskites

1. Introduction

Perovskites-type oxides (ABO_3) with high conductivity are promising candidates as catalysts for solid oxide fuel cells [1] and metal–air batteries [2]. The application of $La_{0.6}Ca_{0.4}CoO_3$ (LCCO) as a bifunctional catalyst, i.e. catalyst for oxygen reduction and evolution for metal–air batteries was applied in rechargeable zinc–air batteries by Müller et al. [3]. To study and compare the mechanism of oxygen reduction/evolution reaction on different perovskites, it is necessary to prepare electrodes on inactive substrates and with well-defined electrolyte/oxide interfaces. Pulsed laser deposition (PLD) has been successfully applied to the growth of many perovskite-type materials [4,5]. During the interaction of a high power density laser with a target, highly excited species are formed in the plasma plume. The chemical state of the plasma exhibits a very dynamic behavior, especially when a reactive gas pulse is applied. The plasma velocity, energy and composition affect the morphological and structural properties of the produced films [4,6]. The dynamics and composition of the plasma have been studied using different experimental methods, such as optical and quadrupole mass spectroscopy, while models have been developed to explain the observed behavior [7]. The properties of the plasma have been measured as a function of

* Corresponding author. Tel.: +41-56-3104076; fax: +41-56-3102485.
E-mail address: thomas.lippert@psi.ch (T. Lippert).

0169-4332/02/$ – see front matter
doi:10.1016/S0169-4332(02)01334-X

time, distance and gas pressure for different atomic species.

The application of pulsed laser deposition in conjunction with a pulsed oxidizing source was developed by Willmott et al. [8] and is called pulsed reactive crossed-beam laser ablation (PRCLA). In this technique, a synchronized pulsed gas source crosses the ablation plume close to its origin, providing an extra degree of freedom in the plume and allowing an increase of gas phase interaction and the probability of reactive scattering, while letting the resulting species propagate freely away from the localized scattering region. The advantage and characterization of this technique have been explained by Willmott et al. [8,9].

The main objective of this experimental study is to analyze the dynamic behavior and composition of the plasma generated during the ablation of LCCO targets in vacuum, O_2 background and with the synchronized N_2O gas pulse under typical growth conditions [10]. A deeper understanding of the plasma dynamics and any correlation with the film properties may allow one to use optical spectroscopy as an in situ diagnostics for thin film growth.

2. Experimental

PRCLA of $La_{0.6}Ca_{0.4}CoO_3$ has been carried out using a KrF excimer laser ($\lambda = 248$ nm, 17 ns pulse length), with a laser fluence of 7.6 J cm^{-2} and a repetition rate of 10 Hz. Two different oxygen sources were used during the experiments: a synchronized pulsed valve operating at a backing pressure of 2 bar N_2O (99.999 % purity, pulse length of 400 μs) and a leak valve to provide an additional background pressure of O_2 of 8×10^{-4} mbar. The time delay between the gas pulse and the laser pulse was 400 μs, where the maximum interaction between the ablation plasma and the gas pulse is achieved.

The plasma formed during the ablation process is analyzed by emission spectroscopy in the range of 300–800 nm. The spectra were collected at different distances from the target (0–10 and 40–50 mm. During deposition, the substrates are typically 45 mm from the target) and different gate delays (0–10 μs) in vacuum, 8×10^{-4} mbar O_2 background pressure, and the same background pressure with the additional N_2O gas pulse. The plasma emission is imaged from the plume via a fiber optic to a spectrometer (Acton Research Corporation Spectra Pro-500) with an I-CCD camera (Princeton Instrument, ICCD-1024-MLDG-E/1, EEV 1024×256 CCD). Two 1.5 mm wide slits in front of the focusing lens define the region of the observed plasma.

3. Results and discussion

Interaction with the gas pulse results in the ablation plume being much brighter and extending further from the target compared to propagation into vacuum or a low-pressure background of O_2 gas. In situ emission spectra of the ablation plume in the range of 300–800 nm are shown in Fig. 1, in vacuum (A), with the O_2 background (B), and with the additional N_2O gas pulse (C). There is only a minimal difference between the spectra A and B. This is not surprising as the mean free path of the plasma particles traveling through the oxygen background is of the order of the vacuum dimensions [8]. The reason why the oxygen is there is merely to provide a sufficient overpressure in order to obtain full oxygen stoichiometry during film growth [11]. The emission lines in the ultraviolet region (300–400 nm), which are associated with higher ionization states of Ca, Co and La, reveal the largest increase in intensity.

There is a large number of lines related to neutral and ionized species of La, Ca and Co, but no peaks due to oxygen or nitrogen are detected. Some spectral lines could not be assigned to the elements and no data were found for emission lines of relevant diatomic species. The emission lines are assigned according to [12] and the analyzed peaks are summarized in Table 1.

Fig. 2 shows the time-resolved emission data corresponding to the emission lines of La II (394.9 nm), Ca I (387.2 nm) and Co I (393.6 nm). The spectra were recorded at different delay times and at a distance of 3 mm from the target in various environments: vacuum, oxygen background and with the additional N_2O gas pulse. Note that different scaling factors have been used for the three environments. It can be clearly seen that the presence of the gas pulse has a strong influence on the observed emission intensity and temporal behavior. A similar effect is detected for all other analyzed elements. The temporal evolution of

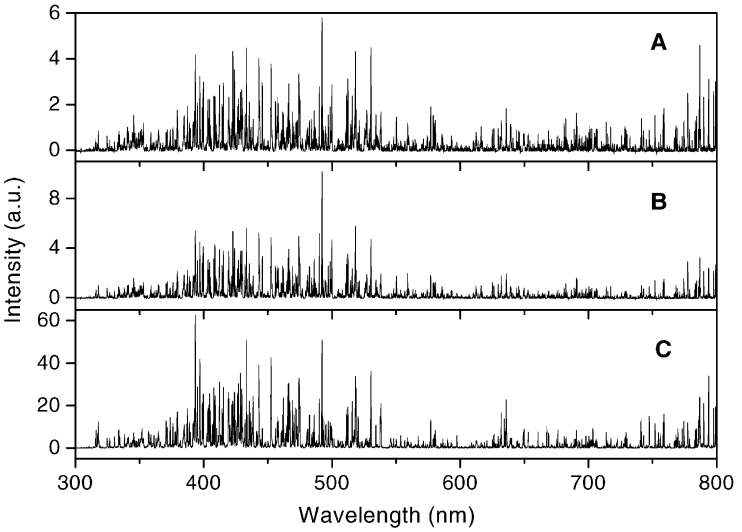

Fig. 1. Emission spectra of $La_{0.6}Ca_{0.4}CoO_3$ from 300 to 800 nm at 3 mm from the target in: (A) vacuum, (B) oxygen background and (C) with additional gas pulse. Note that intensity scales can be directly compared.

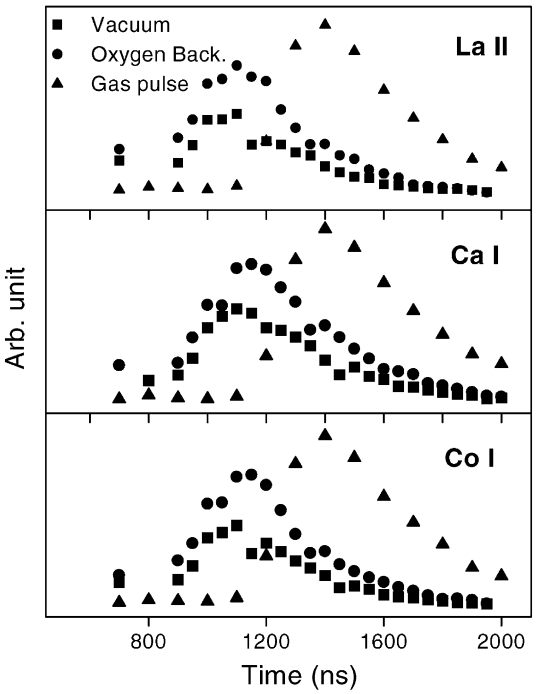

Fig. 2. Time resolved emission data of La II, Ca I and Co I. Note that different scaling factors have been used to allow visual comparison. The following scaling factors (SF) have been applied. Vacuum: La II and Co I SF 5, Ca I SF 4. Oxygen background: La II and Co I SF 10, Ca I SF 7.

the emission observed with the additional gas pulse peaks at later times (approximately 300 ns) and exhibits a long tail. This indicates that the gas pulse plays an important role in the overall creation and decay of the excited states. It is suggested that metastable neutrals and ions are stimulated to luminesce via collisionally induced processes with the gas pulse. These include internal energy redistribution of the plasma species to states with higher emission probabilities, and promotion of electronically low-lying states to higher excited states by collisionally induced ionization and excitation. The increased width of the emission signal when crossed with the gas pulse is therefore a reflection of the time the plasma interacts as it passes through the dense interaction volume of the gas pulse. This has been estimated to have dimensions of the order of 1 cm [8]. The

Table 1
Emission lines and lifetimes for the La, Ca and Co studied in this work

Species	Wavelength (nm)	Lifetime (ns)
La II	394.9	6
Co I	393.6	161
Ca I	387.254	185
	387.256	1.02[a]

[a] The value is in μs.

interaction time is therefore about 1 μs, in good agreement with the observed results.

The timing of the gas pulse and laser trigger means that the plasma expands into the densest part of the gas pulse just as it exits the valve nozzle, where the pressure is about 1 mbar. The velocity of the gas molecules is one order of magnitude smaller than the expanding plasma. Any plasma particle will collide approximately 10 times with molecules of the gas pulse in the initial interaction zone [8]. These collisions between the plasma and the gas particles, where a transfer of internal and kinetic energy will occur, result in a reduced expansion velocity of the plasma particles. For all analyzed elements the maximum emission intensity is 10–40 times higher with the gas pulse compared with vacuum and oxygen background. For the two last conditions, the intensity is of the same order of magnitude, due to the low pressure of the background gas. The increase in the intensity can be attributed to excitation by collisions

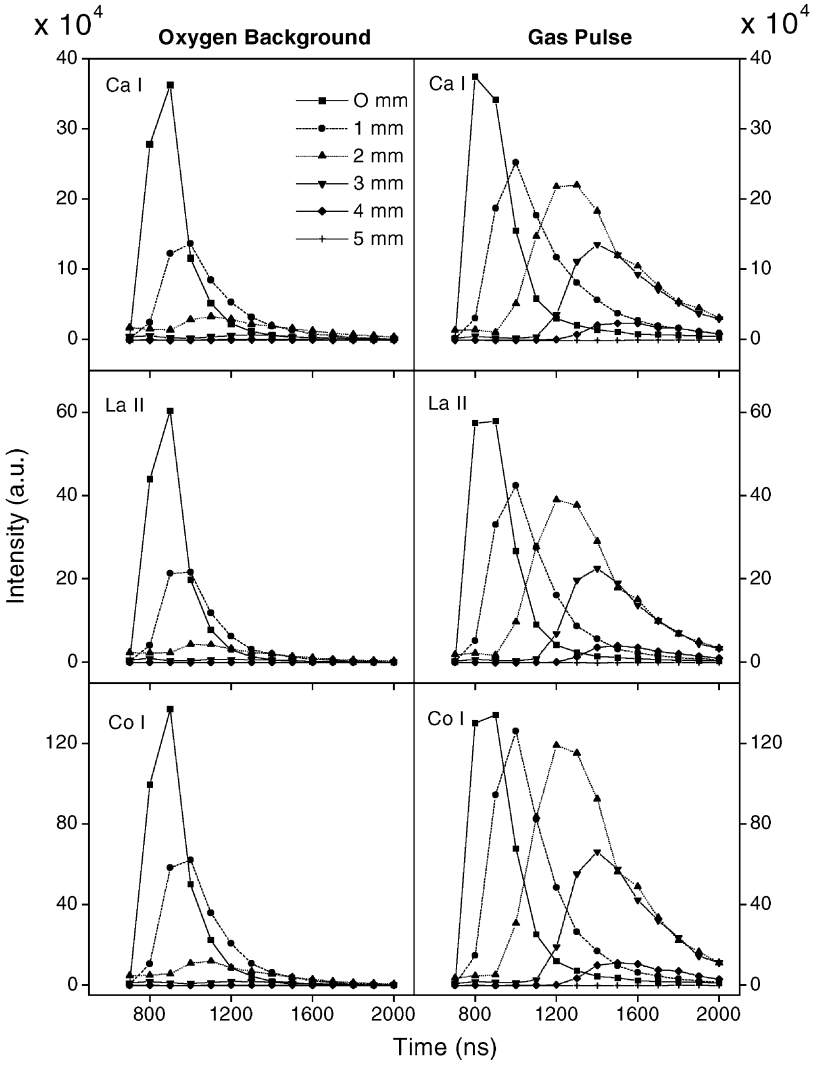

Fig. 3. Time vs. maximum emission intensity of La II, Ca I and Co I at different distances from the target. Left: in oxygen background and; Right: with additional gas pulse.

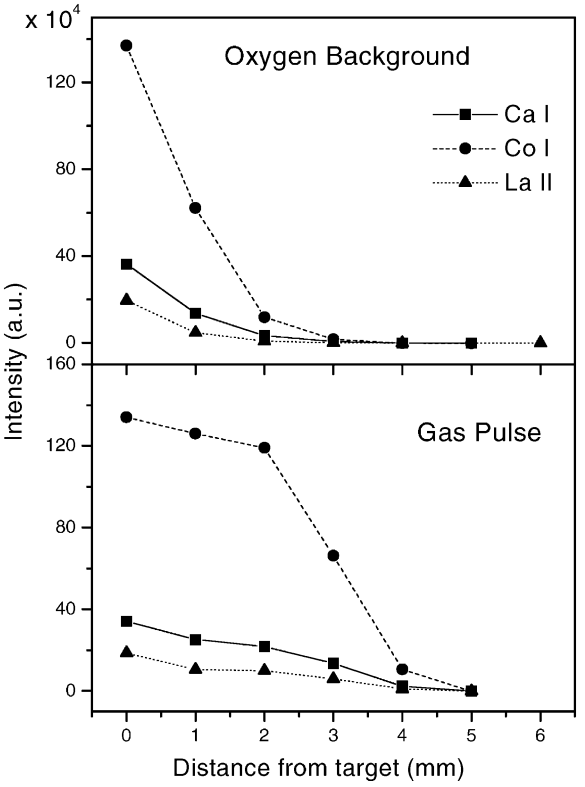

Fig. 4. Maximum intensity vs. distance for Ca I, Co I and La II. Top: in oxygen background and Bottom: with additional gas pulse (lines for guiding the eyes). Note that the origin of the distance scale was the onset of the observed emission signal.

with the gas molecules in the expansion front of the plume (one gas pulse of 400 μs length contains $\sim 10^{17}$ particles). Ionization events and fragmentation reactions during the collisions are expected, but due to the low transition probabilities of the light atoms associated with the gas pulse compared to those of the heavy metallic species originating from the ablation target, they have yet to be detected. It is hoped that they will be established by further experimentation.

Fig. 3 shows the time where the maximum emission intensity is observed, for La II, Ca I and Co I. This dependence is shown at different distances from the target, both in oxygen and with the additional gas pulse. A higher maximum intensity is observed for the gas pulse, occurring at later times. The time of the maximum intensity at a certain distance remains the same for positions within the first 2 mm, both in oxygen background and for the gas pulse. For positions >2 mm, the maximum intensity, obtained with gas pulse, occurs at later times. The lifetime of the excited states of the analyzed species are in the range of several ns to 200 ns (with the exception of one Ca I line which has a lifetime of approximately 1 μs, see Table 1) [12], while the maximum emission in the presence of the gas pulse is observed after delays of several hundred of nanoseconds to a few microseconds. This significant difference indicates that the emission is related to species that have been created significantly after the ablation by collisional excitation with the gas pulse. It is noted that the emission intensity also decreases slightly in the first 1–2 μs due to expansion and dilation of the plasma, though this cannot in general account for the reduction in intensities shown in Fig. 3.

Fig. 4 shows the dependence of the maximum intensity on the distance in oxygen and with the gas pulse. In the presence of oxygen a nearly exponential decay with distance of the excited species produced at the proximity of the target is observed. For the plasma in the presence of the gas pulse this decay is observed further away from the target. In the proximity of the target (around 2 mm) only a small decrease is observed, indicating a quasi equilibrium between the formation and decay of the excited states. After a distance of 2 mm the intensity decays much faster which suggests that the spontaneous emission becomes predominant.

The velocity of the plasma species when interacting with the gas pulse can be inferred from the data shown for Ca I with the gas pulse in Fig. 5. The dependence of distance on time suggests that different processes are active at different distances from the target. Linear fits applied to the two data subsets yield a velocity of 4560 ms^{-1} close to the target and 2000 ms^{-1} further away from the target. The data imply an acceleration in the region between 10 and 40 mm from the ablation target. This behavior is difficult to describe with a delayed shock wave and drag models [13], normally used to fit emission data during PLD in buffer gas. However, as previously quantitatively described, the sudden increase in PRCLA in the degree of ionization due to the plasma-gas pulse interaction causes the plasma potential to rise by several tens of eV as the faster electrons rapidly leave the plasma region,

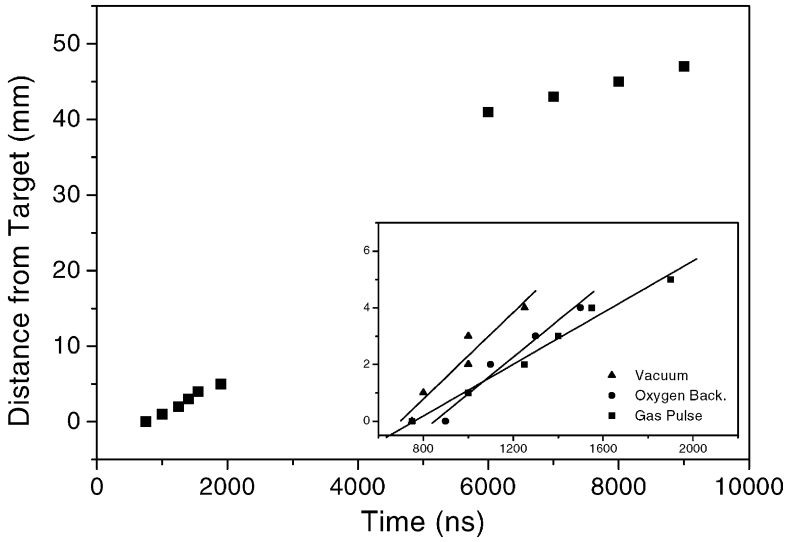

Fig. 5. Time vs. distance of Ca I at the observed maximum intensity for the gas pulse. The insert shows the maximum intensities for the different conditions close to the target.

resulting in a Coulomb explosion [8]. The beneficial effects of the subsequently higher kinetic energies as compared to conventional PLD into a background gas has been discussed in detail elsewhere [9]. Further measurements are needed to establish this hypothesis. The insert in Fig. 5 shows the plasma expansion close to the target in the different environments. The velocity of the plasma particles decreases from vacuum (7600 ms^{-1}) to oxygen background (6500 ms^{-1}) and the additional gas pulse (4600 ms^{-1}). This agrees with the increasing pressure, and therefore the number of collisions (1–2 in the O_2 background and 10 or more with the gas pulse) that will slow down the expanding plasma particles.

4. Conclusions

The presence of the gas pulse has a strong influence on the observed emission intensity and temporal behavior. Higher intensities for the emission lines of all elements are observed. No new emission lines due to the gas pulse interaction can be observed. The time and space resolved measurements reveal that the maximum intensity occurs at later times and can be observed further away from the target. According to these results, the main role of the gas pulse is increasing the collisions between the gas molecules and the plasma particles in a large volume. To explain the mechanisms and dynamic behavior of the plasma with the reactive gas pulse it will be necessary to perform additional experiments and to develop new models.

Acknowledgements

The authors wish to thank Jeff Fuhr of NIST for helpful discussion.

References

[1] J.T. Cheung, P.E.D. Morgan, D.H. Lowndes, X.Y. Zheng, J. Breen, Appl. Phys. Lett. 62 (1993) 2045.
[2] S. Müller, F. Holzer, O. Haas, J. Appl. Electrochem. 28 (1998) 895.
[3] S. Müller, O. Haas, C. Schlatter, C. Comninellis, J. Appl. Electrochem. 28 (1998) 305.
[4] R.A. Gunasekaran, J.D. Pedarnig, M. Dinescu, Appl. Phys. A 69 (1999) 621.
[5] E.A.F. Span, F.J.G. Roesthuis, D.H.A. Blank, H. Rogalla, Appl. Phys. A 69 (1999) S783.
[6] A.M. Haghiri-Gosnet, J. Wolfman, B. Mercey, Ch. Simon, P. Lecoeur, M. Korzenski, M. Hervieu, R. Desfeux, G. Baldinozzi, J. Appl. Phys. 88 (1994) 4257.
[7] J. Gottmann, E.W. Kreutz, Appl. Phys. A 70 (2000) 275.

[8] P.R. Willmott, R. Timm, J.R. Huber, J. Appl. Phys. 82 (1997) 2082.
[9] P.R. Willmott, J.R. Huber, Rev. Mod. Phys. 72 (2000) 1.
[10] M.J. Montenegro, M. Döbeli, T. Lippert, S. Müller, B. Schnyder, A. Weidenkaff, P.R. Willmott, A. Wokaun, Phys. Chem. Chem. Phys. 4 (2002) 2799.
[11] A. Gupta, B.W. Hussey, Appl. Phys. Lett. 58 (1991) 1211.
[12] R.C. Weast, M.J. Astle, W.H. Beyer, Handbook of Chemistry and Physics, Sixty-eighth ed., CRC Press, Boca Raton, FL, 1988.
[13] J. Gonzalo, C.N. Afonso, I. Madariaga, J. Appl. Phys. 81 (1997) 951.